Journal of Alloys and Compounds, 184 (1992) 151–160
JALCOM 191

Synthesis and structure of $Bi_2Fe_2Mn_2O_{10}$

D. M. Giaquinta and H.-C. zur Loye*
Department of Chemistry, Massachusetts Institute of Technology, Cambridge, MA 02139 (USA)

(Received August 23, 1991; in final form November 15, 1991)

Abstract

The crystal structure of a new material, $Bi_2Fe_2Mn_2O_{10}$, in the Bi–Fe–Mn–O system has been determined to be isostructural with $Bi_2Mn_4O_{10}$. Single-crystal studies show the space group to be *Pbam* (No. 55) with unit-cell parameters $a = 7.617(3)$ Å, $b = 8.548(4)$ Å and $c = 5.830(3)$ Å. This new compound has ordered iron and manganese ions in octahedral and square pyramidal sites respectively. This is the first reported example of a quaternary phase with the general structure type of $Bi_2M_4O_{9+\delta}$ (M ≡ Al, Fe, Ga, Mn) having ordered transition metal cations.

1. Introduction

Materials with the general formula $Bi_2M_4O_{9+\delta}$, where M ≡ Al, Fe, Ga and Mn, were first synthesized in 1964 [1–6]. The structural solution was reported in 1968 by Niizeki and Wachi [4], who showed that, while very closely related, the compound $Bi_2Mn_4O_{10}$ is not actually isostructural to the other three compositions, $Bi_2M_4O_9$ (M ≡ Al, Ga, Fe). The two structures differ only in the position of one oxygen atom, which, when M ≡ Al, Fe, Ga, is situated at an inversion center (0, 0, ½). When M ≡ Mn, Niizeki and Wachi found that there is an additional oxygen atom, and the two oxygen atoms are located above and below the inversion center at (0, 0, ±0.281). This extra oxygen atom changes the coordination of two of the manganese ions from tetrahedral to square pyramidal, resulting in two octahedrally and two square pyramidally coordinated manganese ions. Consequently, the general formulae of the two structures may be written as $Bi_2Mn^{oct}{}_2Mn^{sqr\ pyr}{}_2O_{10}$ and $Bi_2M^{oct}{}_2M^{tet}{}_2O_9$ where M ≡ Al, Fe, Ga. The manganese is mixed valent and Bertaut *et al.* [7, 8] have inferred that the manganese(IV) is located on the octahedral sites and manganese(III) is located on the square pyramidal sites.

No ordered quaternary phases of the structure type $Bi_2M_4O_{9+\delta}$ have been synthesized and characterized previously. The solid solution $Bi_2Fe_{4-x}Ga_xO_9$ which has a 60% preferential ordering of iron on the octahedral site [9] has been synthesized in our laboratory and structurally and magnetically characterized. Although the solid solution $Bi_2Fe_{4-x}Mn_xO_{9+\delta}$ has been reported

*Author to whom correspondence should be addressed.

0925-8388/92/$5.00

in the literature [3, 6], the materials were only poorly characterized and the results were conflicting. According to Masuno [3], there exists only limited miscibility on either side of the phase diagram, where $0 \leqslant x \leqslant 0.9$ and $3.6 \leqslant x \leqslant 4.0$, while in the center a multiphase region exists containing $Bi_2Fe_4O_9$, $Bi_2Mn_4O_{10}$ and Bi(Fe, Mn)O_3. According to Jimenez [6], a complete solid solution exists across the entire range of x; however, it was assumed that the two end members were actually isostructural, and therefore that their X-ray powder diffraction patterns were identical. This assumption is incorrect since, upon altering the oxygen coordination, both the structure and the powder pattern change appreciably. In our laboratory the solid solution $Bi_2Fe_{4-x}Mn_xO_{9+\delta}$ is currently being investigated across the entire range of x, in order to characterize fully the materials structurally and magnetically in the light of the structural and magnetic in formation which we recently obtained about the solid solution $Bi_2Fe_{4-x}Ga_xO_9$ [9]. We present here the synthesis and structure of the ordered material $Bi_2Fe_2Mn_2O_{10}$, as determined by single-crystal X-ray diffraction.

2. Experimental details

Crystals of $Bi_2Fe_2Mn_2O_{10}$ were grown in a Bi_2O_3 flux using stoichiometric amounts of Fe_2O_3 (Cerac 99.99%) and Mn_2O_3 (Cerac 99.99%) in a fivefold excess of Bi_2O_3 (Cerac 99.9%). The resulting 12 g charge was thoroughly mixed in a platinum crucible and heated at 5 °C min^{-1} to 1000 °C. The flux was soaked for 24 h and slowly cooled at a rate of 5 °C h^{-1} to 700 °C. The flux was then rapidly cooled to room temperature. The black shiny crystalline product was separated from the flux matrix by dissolving the flux in dilute HNO_3. Single crystals which grew as prisms, some up to 1 mm on edge, were isolated with a dissecting probe.

The crystals obtained from the flux growth were first analyzed by precession photographs using a Charles Supper Co. precession camera with a crystal-to-film distance of 59 mm, and a precession angle of 10° mounted on an Enraf–Nonius 581 Diffractis X-ray generator. Careful selection enabled a single crystal to be chosen for structure solution. The diffraction patterns of the precession photographs were consistent with the structure of the related $Bi_2Mn_4O_{10}$; however, the calculated lattice parameters differed. Energy-dispersive spectroscopy was performed to confirm the presence of bismuth, iron and manganese using the same crystal that was used for the structure analysis. Wavelength-dispersive spectroscopy performed using a JEOL 781 microprobe on six representative crystals, having a theoretical composition of $Bi_2Fe_2Mn_2O_{10}$, yielded an average composition of $Bi_2Fe_{2.1}Mn_{1.9}O_{10}$.

A crystal of $Bi_2Fe_2Mn_2O_{10}$ having the approximate dimensions 0.060 mm × 0.050 mm × 0.040 mm was chosen for the single-crystal structure solution. All measurements were made on a Rigaku AFC6R diffractometer with graphite monochromated Mo Kα radiation ($\lambda = 0.71069$ Å) and a 12 kW rotating-anode generator. Crystallographic data are summarized in Table 1.

TABLE 1

Summary of crystallographic data for $Bi_2Fe_2Mn_2O_{10}$

Empirical formula	$Bi_2Fe_2Mn_2O_{10}$
Formula weight	799.52
Crystal color, habit	Black, prismatic
Crystal dimensions (mm×mm×mm)	0.060×0.050×0.040
Crystal system	Orthorhombic
Space group	*Pbam* (No. 55)
Number of reflections used for unit cell Determination (2θ range)	24 (12.8°–27.3°)
ω scan peak width at half-weight	0.30
Lattice parameters (Å)	
a	7.617 (3)
b	8.548 (4)
c	5.830 (3)
Volume (Å^3)	379.6(3)
Z	2
D_{calc} (g cm^{-3})	6.994
F_{000}	696
Diffractometer	Rigaku AFC6R
Radiation	Mo Kα (λ=0.710 69 Å)
$\mu_{(Mo\ K\alpha)}$ (cm^{-1})	529.43
Temperature (°C)	23
Scan type	ω–2θ
$2\theta_{max}$	54.9°
Number of reflections measured	549
Number of observations ($I>3.00\sigma(I)$)	358
Number of variables	31
Corrections	Lorentz–polarization Absorption (transmission factors, 0.72–1.41) Secondary extinction (coefficient, 0.552 08×10^{-6})
Residuals R, R_w	0.042; 0.052
Goodness-of-fit indicator	1.82
Maximum peak in final difference map (e$^-$ Å^{-3})	3.69

Cell constants and an orientation matrix for data collection, obtained from a least-squares refinement using the setting angles of 24 carefully centered reflections in the range of $12.79<2\theta<27.30°$ correspond to an orthorhombic cell with the dimensions $a=7.617(3)$ Å, $b=8.548(4)$ Å, $c=5.830(3)$ Å and $V=379.6(3)$ Å^3. For $Z=2$ and the formulation weight 799.52, the calculated density is 6.994 g cm^{-3}. Based on the systematic absences of $0kl$, $k\neq 2n$, and $h0l$, $h\neq 2n$, packing considerations, a statistical analysis of intensity distribution and the successful solution and refinement of the structure, the space group was determined to be *Pbam* (No. 55).

The data were collected at a temperature of 23±1 °C, using the ω–2θ scan technique to a maximum 2θ value of 54.9°. ω scans of several intense

reflections, made prior to data collections, had an average width at half-height of 0.30° with a take-off angle of 6.0°. Scans of $(1.21+0.35 \tan \theta)°$ were made at a speed of 8.0° min^{-1} (in ω). The weak reflections ($I < 10.0\sigma(I)$) were rescanned (maximum of eight rescans) and the counts were accumulated to assure good counting statistics. Stationary background counts were recorded on each side of the reflection. The ratio of peak counting time to background counting time was 2 to 1. The diameter of the incident beam collimator was 0.5 mm and the crystal-to-detector distance was 310.0 mm. A total of 549 reflections were collected. The intensities of three representative reflections which were measured after every 150 reflections remained constant throughout data collection indicating crystal and electronic stability (no decay correction was applied). Data were corrected for Lorentz, polarization, absorption [10] and secondary extinction. Data were empirically corrected for absorption by means of the DIFABS program [11].

All calculations were carried out on a Micro VAX 3500 with the use of TEXSAN crystallographic software [12]. The structure was solved by direct methods [13]. Refinement was performed using a full-matrix least-squares calculation. The final values of the discrepancy factors were $R=0.042$ ($R=\Sigma||F_o|-|F_c||/\Sigma|F_o|=0.042$) and $R_w=0.052$ ($R_w=[(\Sigma w(|F_o|-|F_c|)^2/\Sigma wF_o^2)]^{1/2}=0.052$), $w=4F_o^2/\sigma^2(F_o^2)$. The goodness of fit was 1.82 and the highest peak in the final difference map was 3.69 e^- $Å^{-3}$. The atomic scattering factors were those of Cromer and Waber as were the corrections for anomalous dispersions [10, 14].

3. Results

Final atomic positions and anisotropic U values are listed in Tables 2 and Table 3 respectively. Selected interatomic distances are listed in Table 4. A view parallel to the a–b plane of $Bi_2Fe_2Mn_2O_{10}$ is shown in Fig. 1 (the Bi–O bonds have been omitted for clarity). It consists of columns of edge-sharing octahedra which are corner shared with edge-sharing square pyramids as shown in an expanded view in Fig. 2. The octahedra are located in layers that are separated by doubly packed square pyramidal layers. These layers

TABLE 2

Positional and isotropic equivalent thermal parameters

Atom	x	y	z	B(eq)
Bi	0.15798(12)	0.16424(13)	0	0.74(5)
Fe	½	0	0.2574(6)	0.3(1)
Mn	0.3924(5)	0.3489(5)	½	0.7(1)
O(1)	0	0	0.291(4)	1.7(4)
O(2)	0.384(2)	0.200(2)	0.250(2)	1.0(2)
O(3)	0.639(2)	0.078(2)	½	1.1(3)
O(4)	0.156(2)	0.441(2)	0	0.3(3)

TABLE 3

u_{ij} or U values ($\times 100$) for $Bi_2Fe_2Mn_2O_{10}$

Atom	u_{11} (U) ($Å^2$)	u_{22} ($Å^2$)	u_{33} ($Å^2$)	u_{12} ($Å^2$)
Bi	0.93(6)	0.96(6)	0.94(6)	0.11(4)
Fe	0.19(13)	0.5(2)	0.4(2)	0.1(2)
Mn	1.4(2)	0.9(2)	0.3(2)	0.5(2)
O(1)	2.2(5)			
O(2)	1.3(3)			
O(3)	1.3(4)			
O(4)	0.4(4)			

TABLE 4

Bond distances for metal atoms in $Bi_2Fe_2Mn_2O_{10}$

Atom	Atom	Distance (Å)	Atom	Atom	Distance (Å)
Bi	O(1)	2.508(15)	Fe	O(4)	1.978(11)
Bi	O(2)	2.275(13)	Fe	Fe	2.829(7)
Bi	O(4)	2.369(18)	Fe	Fe	3.001(7)
Bi	O(4)	2.375(17)	Fe	Mn	3.401(5)
Bi	Fe	3.318(2)	Fe	Mn	3.550(4)
Bi	Fe	3.455(2)	Mn	O(1)	1.957(14)
Bi	Mn	3.550(3)	Mn	O(2)	1.940(14)
Fe	O(2)	1.923(14)	Mn	O(3)	2.026(19)
Fe	O(3)	1.891(13)			

form slabs of alternating octahedral–square pyramidal–octahedral coordination. The slabs in turn are separated from each other by planes of bismuth and oxygen which are regularly modulated in the ***b*** direction (Fig. 3). The octahedra are connected across the square pyramid and bismuth oxide layer via edge-sharing oxygen atoms located in the square pyramidal and bismuth oxide plane respectively.

The two coordination sites in the structural solution were analyzed with iron and manganese in both sites and with both iron and manganese mixed in a single site. The site multiplicities were refined and the residual values that resulted from these refinements were found to be lowest when the iron and manganese were placed only on the octahedral and square pyramidal site respectively.

The iron octahedra are slightly tetragonally distorted, the longest bond being only 0.09 Å longer than the shortest bond, which point toward the bismuth oxide plane and the next edge-shared octahedron respectively. The Fe–O bond which corner shares with the square pyramids is slightly bent toward the square pyramid, which are virtually undistorted in bond lengths and angles; the apical oxygen bond is 0.09 Å longer than the basal oxygen

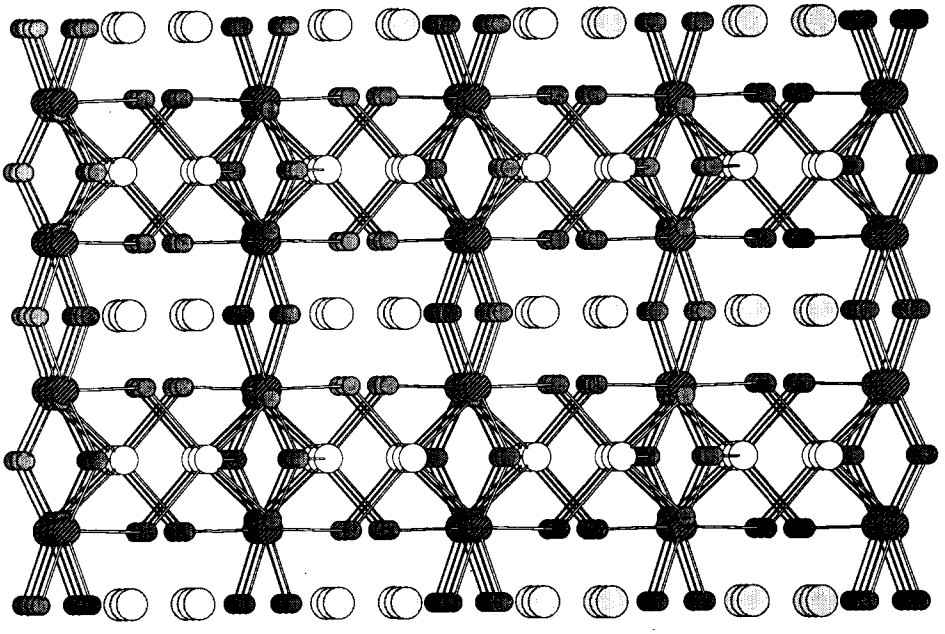

Fig. 1. A view of $2\times2\times2$ unit cells of $Bi_2Fe_2Mn_2O_{10}$ parallel to the a–b plane: ◎, bismuth; ◍, iron; ○, manganese; ●, oxygen.

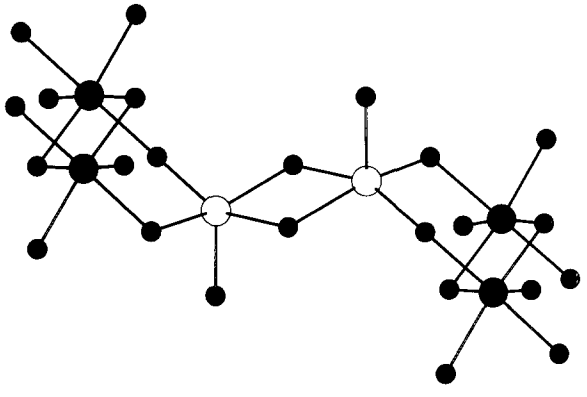

Fig. 2. A view of edge-shared octahedral positions and edge-shared square pyramidal positions.

bonds. The bismuth atoms are located at the apices of trigonal pyramids formed by three Bi–O bonds of varying lengths from 2.27 to 2.38 Å. If second- and third-nearest neighbors are included, the bismuth ions are surrounded by ten oxygen atoms. All oxygen atoms in the structure are tetrahedrally coordinated.

A view perpendicular to the a–b plane (Fig. 3) shows a complicated packing network of distorted ten-membered rings of metal and oxygen atoms.

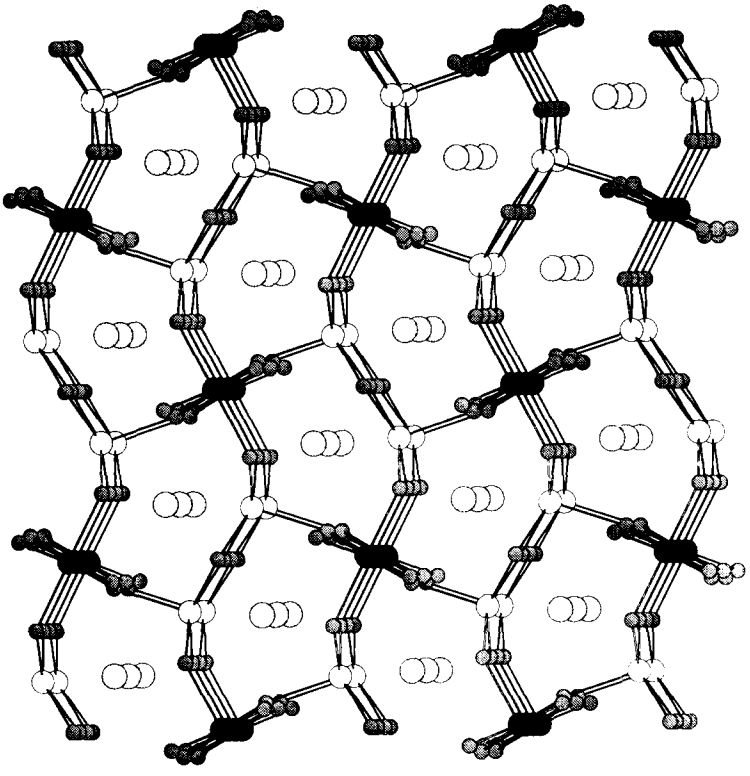

Fig. 3. A view perpendicular to the *a*–*b* plane with distorted ten-membered rings. The order of planes going into the page is bismuth–octahedral sites–square pyramidal sites–octahedral sites–bismuth (Bi–O bonds have been omitted for clarity). Note the modulation in the *b* direction.

The tenfold rings are made up of polygons in repeating groups of octahedron–square pyramid–square pyramid–octahedron–square pyramid. The two middle square pyramids are edge shared with each other; however, the remaining contacts are via corners. The order of planes going into the page is bismuth–octahedral sites–square pyramidal sites–octahedral sites–bismuth (the Bi–O bonds have been omitted for clarity).

4. Discussion

The manganese in the $Bi_2Mn_4O_{10}$ structure is mixed valent, manganese(III) and manganese(IV), with the two oxidation states of manganese segregated in square pyramidal and octahedral coordination, respectively [7, 8]. This assignment, based on bond lengths, places the manganese(IV) into a site different from what we found in the isostructural $Bi_2Fe_2Mn_2O_{10}$, where manganese(IV) is located in the square pyramidal site instead. Mn(IV) d^3 in an octahedral site should result in an undistorted octahedron, similar to that

found in $Bi_2Fe_4O_9$, where Fe(III) d^5 occupies the octahedral position. The structural distortion which is observed in the octahedral site of $Bi_2Mn_4O_{10}$ could be explained by assigning the Jahn–Teller ion manganese(III) to the octahedral site instead; this would place manganese(IV) onto the square pyramidal site, in agreement with our structure. Although manganese(III) may prefer square pyramidal geometry over manganese(IV) in some cases, manganese(IV) is not normally found in the distorted octahedral geometry seen in $Bi_2Mn_4O_{10}$. Supporting this assignment is the fact that in $Bi_2Fe_2Mn_2O_{10}$ the octahedral sites are fairly undistorted as they are in $Bi_2Fe_4O_9$. The $Bi_2Mn_4O_{10}$ structure was refined to an R value of only 11%, however, making it difficult to assign unambiguously the coordination of manganese(III) *vs.* manganese(IV) based on the observed distortions. We are planning to carry out Mössbauer studies to determine definitively the iron coordination across the entire solid solution $Bi_2Fe_{4-x}Mn_xO_{9+\delta}$.

Comparing the structure of $Bi_2Fe_2Mn_2O_{10}$ with that of $Bi_2Mn_4O_{10}$ we find that the square pyramid is more regular in $Bi_2Fe_2Mn_2O_{10}$ than in $Bi_2Mn_4O_{10}$. The four lengths in the basal plane are all equal, unlike in $Bi_2Mn_4O_{10}$, where one side of the base is longer than both the opposite side and the apical bond (Table 5). The base plane angles are slightly contracted toward the edge-shared (square pyramidal) direction and expanded in the corner-shared (octahedral) direction. The apical metal–oxygen bond is approximately 0.1 Å longer than the metal–oxygen bond in the base plane.

In $Bi_2Fe_2Mn_2O_{10}$ the octahedra are occupied strictly by iron atoms, suggesting that certain similarities should exist between the octahedral sites in $Bi_2Fe_2Mn_2O_{10}$ and those in $Bi_2Fe_4O_9$. The octahedral bond lengths are, in fact, close to those present in $Bi_2Fe_4O_9$, except for those which are shared between octahedra and square pyramids; these bonds are more akin to those found in $Bi_2Mn_4O_{10}$, where the basal plane of the square pyramid contacts more closely with the octahedra as compared to a tetrahedral–octahedral contact. Also, the octahedral angles in $Bi_2Fe_2Mn_2O_{10}$ are more akin to those found in the all iron compound than in the all manganese compound. The O(3)–Fe–O(4) angle is the widest found in all the compounds. O(4) is located in the Bi–O layer, while O(3) is an edge-shared octahedral oxygen atom as well as the apical oxygen atom for the square pyramid. The angle is widened because, unlike the situation in the all-iron compound, O(3) is attached to a square pyramid, which has a broader basal plane than the tetrahedron found in $Bi_2Fe_4O_9$. In $Bi_2Mn_4O_{10}$, on the contrary, the octahedra are more strongly distorted, unlike the more ideal situation found in $Bi_2Fe_2Mn_2O_{10}$.

The Bi–O planes are regularly modulated in the $\boldsymbol{b}$ direction, as has been seen in other layered bismuth oxides [15]. The modulation is more pronounced in $Bi_2Fe_2Mn_2O_{10}$ than in either $Bi_2Fe_4O_9$ or $Bi_2Mn_4O_{10}$. This is caused by the insertion of the extra oxygen atom to make edge-sharing square pyramids, which allows a smoother modulation relative to corner-sharing tetrahedra. The absence of a distortion in the $Bi_2Fe_2Mn_2O_{10}$ octahedra also contributes to the enhanced modulation.

TABLE 5

Comparison of cation coordination angles and bond lengths

	Octahedral angle (deg)			
	$Bi_2Mn_4O_{10}$[a]	$Bi_2Fe_4O_9$[a]	$Bi_2Fe_2Mn_2O_{10}$	$Bi_2Fe_2Ga_2O_9$[b]
O(3)–M–O(4)	96.1	97.4	98.2	96.4
O(4)–M–O(4)	80.5	82.1	81.2	83.0
O(2)–M–O(3)	93.4	92.7	94.4	95.4
O(2)–M–O(4)	88.4	91.0	91.8	91.9
O(2)–M–O(3)	89.9	88.8	87.8	89.0
O(2)–M–O(4)	88.1	87.4	86.0	83.6
	Octahedral length (Å)			
	$Bi_2Mn_4O_{10}$	$Bi_2Fe_4O_9$	$Bi_2Fe_2Mn_2O_{10}$	$Bi_2Fe_2Ga_2O_9$
M–O(2)	1.83	1.95	1.923(14)	2.025(13)
M–O(3)	1.90	1.95	1.891(13)	1.951(14)
M–O(4)	1.98	2.05	1.978(11)	2.041(14)

	Square pyramidal angle (deg)	
	$Bi_2Mn_4O_{10}$	$Bi_2Fe_2Mn_2O_{10}$
O(1)–Mn–O(1)	82.9	77.0
O(2)–Mn–O(2)	86.7	97.6
O(3)–Mn–O(1)	97.0	101.4
O(3)–Mn–O(2)	100.4	99.8
O(1)–Mn–O(2)	92.6	88.8
	Square pyramidal length (Å)	
	$Bi_2Mn_4O_{10}$	$Bi_2Fe_2Mn_2O_{10}$
Mn–O(1)	1.91	1.957(14)
Mn–O(2)	2.10	1.940(14)
Mn–O(3)	2.04	2.026(19)

[a]Values from Niizeki and Wachi [4]; the final R values are 0.11 and 0.10 for the manganese and iron compounds respectively.
[b]Values from Giaquinta *et al.* [9]; the final R value is 0.053.

5. Conclusions

The crystal structure of $Bi_2Fe_2Mn_2O_{10}$ was determined by single-crystal X-ray diffraction. The structure has ordered transition metals which are located in octahedral and square pyramidal sites for iron and manganese respectively. This is the first truly ordered compound with the $Bi_2M_4O_{9+\delta}$, (M≡Al, Fe, Ga, Mn) structure. Since iron(III) is located only on octahedral sites, there is no Jahn–Teller distortion of the octahedra as is observed in $Bi_2Mn_4O_{10}$.

The oxidation state of the manganese is +4, accounting for the extra oxygen atom found in $Bi_2Fe_2Mn_2O_{10}$ *vs.* $Bi_2Fe_4O_9$. The Bi–O planes are regularly modulated in the ***b*** direction as has been seen in other layered bismuth oxides. This modulation is more pronounced in $Bi_2Fe_2Mn_2O_{10}$ than in either $Bi_2Fe_4O_9$ or $Bi_2Mn_4O_{10}$.

Acknowledgments

We thank W. M. Davis of the Single-Crystal X-ray Diffraction Facility, Massachusetts Institute of Technology, Department of Chemistry, for collecting the crystallographic data set. This work was supported by the Massachusetts Institute of Technology, Center for Material Science and Engineering, under Grant DMR 9022933.

References

1 H. Koizumi, N. Niizeki and T. Ikeda, *Jpn. J. Appl. Phys.*, *3* (1964) 495.
2 A. G. Tutov, I. E. Myl'nikova, N. N. Parfenova, V. A. Bokov and S. A. Kizhaev, *Sov. Phys.—Solid State*, *6* (1964) 963.
3 K. Masuno, *Nippon Kagaku Zasshi*, *88* (1967) 726.
4 N. Niizeki and M. Wachi, *Z. Kristallogr.*, *127* (1968) 173.
5 A. G. Tutov and V. N. Markin, *Neorg. Mater.*, *6* (1970) 2014.
6 C. M. Jimenez, *Bol. Soc. Esp. Ceram. Vidrio*, *17* (1978) 365.
7 E. F. Bertaut, G. Buisson and S. Quezel-Ambrunaz and G. Quezel, *Solid State Commun.*, *5* (1967) 25–30.
8 E. F. Bertaut, G. Buisson and S. Quezel-Ambrunaz, *C.R. Acad. Sci., Paris*, *258* (1964) 3025.
9 D. Giaquinta, G. C. Papaefthymiou, W. M. Davis and H.-C. zur Loye, *J. Solid State Chem.*, (1992), in press.
10 D. T. Cromer and J. T. Waber, in J. A. Ibers and W. C. Hamilton (eds.), *International Tables for X-ray Crystallography*, Kynoch Press, Birmingham, 1974, Table 2.2A.
11 N. Walker and D. Stuart, *Acta Crystallogr., Sect. A*, *39* (1983) 158.
12 P. N. Swepston, *TEXSAN*; version 5.1, Molecular Structure Corporation, College Station, TX, 1986.
13 C. J. Gilmore, *J. Appl. Crystallogr.*, *17* (1984) 42.
14 D. T. Cromer and J. T. Waber, in J. A. Ibers and W. C. Hamilton (eds.), *International Tables for X-ray Crystallography*, Kynoch Press, Birmingham, 1974, Table 2.3.1.
15 J. M. Tarascon, Y. LePage and W. R. McKinnon, *Eur. J. Solid State Inorg. Chem.*, *27* (1990) 81.